

Land-Coverage Aware Path-Planning for Multi-UAV Swarms in Search and Rescue Scenarios

Pedro Antonio Alarcon Granadeno¹ and Jane Cleland-Huang²

Abstract— Unmanned Aerial Vehicles (UAVs) have become vital in search-and-rescue (SAR) missions, with autonomous mission planning improving response times and coverage efficiency. Early approaches primarily used path planning techniques such as A*, potential-fields, or Dijkstra’s algorithm, while recent approaches have incorporated meta-heuristic frameworks like genetic algorithms and particle swarm optimization to balance competing objectives such as network connectivity, energy efficiency, and strategic placement of charging stations. However, terrain-aware path planning remains under-explored, despite its critical role in optimizing UAV SAR deployments. To address this gap, we present a computer-vision based terrain-aware mission planner that autonomously extracts and analyzes terrain topology to enhance SAR pre-flight planning. Our framework uses a deep segmentation network fine-tuned on our own collection of landcover datasets to transform satellite imagery into a structured, grid-based representation of the operational area. This classification enables terrain-specific UAV task allocation, improving deployment strategies in complex environments. We address the challenge of irregular terrain partitions, by introducing a two-stage partitioning scheme that first evaluates terrain monotonicity along coordinate axes before applying a cost-based recursive partitioning process, minimizing unnecessary splits and optimizing path efficiency. Empirical validation in a high-fidelity simulation environment demonstrates that our approach improves search and dispatch time over multiple meta-heuristic techniques and against a competing state-of-the-art method. These results highlight its potential for large-scale SAR operations, where rapid response and efficient UAV coordination are critical. For additional supplementary materials please see <https://github.com/SAREC-Lab/terrain-aware-planning>

I. INTRODUCTION

Over the past years, there has been significant advances in autonomous SAR mission planners tailored for UAVs. Early solutions primarily leveraged heuristic methods, such as A*, potential fields, and optimal search algorithms like Dijkstra’s, to compute deterministic, collision-free paths while minimizing path cost to guarantee deterministic, collision-free paths while minimizing path length. Building upon these foundations, researchers introduced metaheuristic algorithms like genetic algorithms [1], [2], ant colony optimization [3], and particle swarm optimization to concurrently address competing UAV-assisted SAR objectives, such as network connectivity, energy efficiency, and the strategic placement

^{*}This work was supported by the USA National Science Foundation under Grant 1931962

¹Pedro Antonio Alarcon Granadeno is a PhD student in the Computer Science and Engineering department at the University of Notre Dame, IN, USA palarcon@nd.edu

²Jane Cleland-Huang is a Professor in the Department of Computer Science and Engineering, University of Notre Dame, IN, USA JaneHuang@nd.edu

of charging stations around the search area. More recently, hybrid approaches [4], [5] have been proposed that blend classical heuristics, metaheuristic frameworks, and AI-based strategies to leverage their complementary strengths.

While significant progress has been made in UAV-assisted SAR cooperation, relatively little attention has been given to autonomous terrain-based path planning. Terrain is a crucial factor influencing search priorities. For example, in large-scale earthquakes, locating survivors often hinges on building-centric searches due to structural collapses and high casualty rates in dense urban areas. Similarly, in missing-person cases in rugged wilderness, prior incidents [6] show that healthy adults tend to follow trails, roads, or other linear features. Terrain-awareness provides critical information for allocating heterogeneous UAVs with varying capabilities, sensors, and payloads. For instance, LiDAR-equipped UAVs excel in dense forests or tightly spaced buildings, while multispectral and polarimetric cameras, resistant to reflective glare, are ideal for waterbodies. However, terrain-based prioritization and resource allocation have traditionally relied on manual satellite analysis and ground surveys, hindering efficiency and limiting UAV scalability, even when rapid, large-scale response is imperative.

To address this, we propose a Computer-Vision (CV) based terrain-aware mission planner that autonomously extracts and analyzes terrain topology for SAR mission planning. In contrast to conventional approaches that rely on manual terrain analyses, our framework leverages a deep segmentation network, fine-tuned on landcover datasets, which transforms high-resolution satellite imagery into a grid-based representation of the operational area, where landcover types are represented as disjoint rectilinear polygons.

A key challenge in this approach is that real-world terrain features produce irregular rectilinear polygons with diverse concavities, holes, and varying sizes. Traditional Coverage Path Planning (CPP) methods [7], [8] applied to such complex polygons often employ excessive partitioning to enforce convexity, resulting in increased path lengths and UAV travel times (a consequence that could be life-threatening in emergency response scenarios). While metaheuristic approaches can avoid explicit partitioning, they frequently yield suboptimal paths. To mitigate these inefficiencies, we introduce a novel partitioning scheme that operates in two stages. First, our method assesses whether partitioning is necessary by evaluating the polygon’s monotonicity along both coordinate axes. If further division is warranted, a cost function based on gap severity guides a recursive partitioning process. Taken together, our work presents a terrain-aware mission planning

framework that reduces reliance on manual terrain analysis and enhances UAV coverage and efficiency.

The remainder of the paper is structured as follows. Section II discusses related work on autonomous SAR mission planning, surveying both classical heuristic methods and recent advances that incorporate metaheuristic and AI-based strategies. Section III details our proposed algorithm, including 2D scene reconstruction using segmentation techniques, and our novel coverage path planning method, including the two-stage partitioning scheme and candidate path generation, and then introduces a UAV-task matchmaking algorithm that aligns platform capabilities with terrain-specific requirements. Section V presents an evaluation of our framework via a prototype implementation in a high-fidelity simulation environment, and Section VI summarizes outcomes and discusses directions for future research.

II. RELATED WORK

A. Autonomous Path Planners in Search and Rescue

Prior path planning approaches for autonomous UAV Search and Rescue (SAR) operations has focused on classical planners, metaheuristic approaches, and hybrid techniques [9]. Classical approaches, i.e. A*, Dijkstra's algorithm, RRT, and potential field methods, are well-known for their deterministic behavior and ease of implementation; however they are primarily designed to optimize a single objective, typically minimizing path length or travel cost, with obstacle avoidance enforced as a constraint. This narrow focus neglects other key aspects, such as energy efficiency, UAV-failures, network connectivity, and/or heterogeneity of UAV fleet. In addition, they generally require significant computational resources for large search spaces [10].

Researchers have increasingly turned to metaheuristic methods, such as genetic algorithms (GAs), ant colony optimization (ACO), particle swarm optimization (PSO) and simulated Annealing (SA) to address these weaknesses as they are well-suited for multi-objective optimization, allowing for the concurrent minimization of several competing cost functions. For instance, [1], [2] uses a GA to optimize UAV flight paths by minimizing a fitness function that considers mission completion time, high-priority area coverage, network-connectivity, penalties for energy violations, and charging station placement. [3] uses ACO to optimize a cumulative probability of success through balancing target detection probability and target presence likelihood—modeled via a Markovian motion model and sensor performance law. Despite their flexibility, their performance is highly sensitive to hyperparameter tuning, whereby minor misconfigurations can significantly impede convergence and degrade solution quality as shown in [3]. Additionally, meta-heuristics are generally iterative and computationally heavier than one-shot classical methods, which require many candidate solutions over numerous generations/iterations to converge. Hence, they generally exponentially grow with an increasingly large operational area and quickly become infeasible for real-time operations. This also makes them susceptible to uncertain

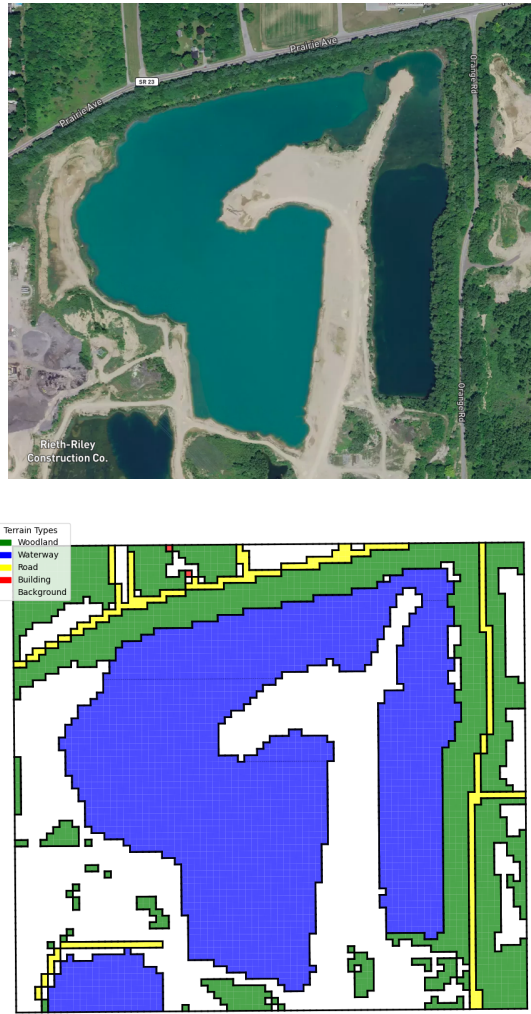


Fig. 1: (top) Raw high-resolution satellite image used as input for scene reconstruction. (bottom) Terrain-labeled rectilinear polygons produced via segmentation and DFS-based connected component extraction.

dynamic environments not accounted for in the original parameter formulation (e.g. UAV hardware failure).

More recently, hybrid approaches have emerged as the preferred candidates for UAV path planners. Hybrid approaches combine different techniques (e.g. classical, AI, meta-heuristics, global planners, local planners, etc.) to leverage their complimentary strengths. For instance, [4], proposed a hybrid PSO algorithm called PPSwarm that first employs RRT* to rapidly find an initial feasible route for each UAV, then uses PSO to iteratively optimize a path based on path length and hazard zones. Hybrid systems sometimes use classical algorithms for high-level planning and metaheuristics for local adjustments (or vice versa). For instance, [5] proposed a hybrid UAV path planning framework that first uses a global static planner based on the A* algorithm to compute an optimal route in a known environment, then refine it with a local dynamic planner using Q-Learning, which adapts the path in real time to

account for dynamic obstacles and environmental changes. Drawbacks include increased system complexity, with techniques sometimes inheriting drawbacks of their constituent techniques (e.g. global planners like A* can be rigid when faced with sudden environmental changes).

Many existing planners largely overlook landcover topology, despite its important for SAR planning, often relying on time-consuming manual inputs to define terrain-based strategies. To bridge this gap, we propose a hybrid autonomous UAV-assisted SAR mission generator that subdivides planning into global and local stages. For global planning, the operational area is segmented into terrain-based rectilinear polygons that are dynamically allocated among available UAVs, considering factors such as landcover priority, proximity, and UAV heterogeneity (i.e. varying capabilities, payloads, and sensor configurations). In local planning, we implement a novel polygon decomposition strategy to construct boustrophedon-based paths that optimize both path length, number of turns and mission completion time. This explicit consideration of terrain factors addresses a gap in contemporary literature and lays the foundation for more informed, autonomous SAR operations.

B. Polygon Decomposition for Coverage Path Planning

The pipeline of Coverage Path Planning (CPP) for polygons often begins with polygon decomposition schemes to partition areas into disjoint convex polygons. The three best established partitioning algorithms are trapezoidal, Morse-based [11] and boustrophedon cell decomposition strategies [7]. They all fundamentally leverage a line-sweep mechanism which partitions the environment by detecting changes in free-space connectivity; however, they adopt various partitioning *criteria*. In the trapezoidal method, a vertical sweep line tracks intersections with obstacle edges and introduces a partition at every change, yielding convex cells that are straightforward to cover but are often overly segmented. Similarly, Morse-based decomposition employs a real-valued Morse function to pinpoint critical points where the gradient vanishes and connectivity shifts, generalizing the notion of connectivity-based partitioning but still risking excessive subdivisions. In contrast, boustrophedon decomposition prioritizes maintenance of free-space monotonicity with respect to the sweep line direction, resulting in continuous sweep segments in the orthogonal direction.

Our partitioning scheme most closely resembles the traditional boustrophedon cell decomposition strategy [7], where a sweep line is used to detect changes in the free space's connectivity, determining whether the region is monotone with respect to the sweep direction. However, unlike the boustrophedon decomposition strategy, which triggers partitioning solely on connectivity changes, our approach employs a *cumulative gap severity* cost function that quantifies the cost incurred by concavities and selectively partitions along the maximum gap value. Furthermore, partitioning is only triggered when a polygon exhibits non-monotonicity in **both** directional axes, which minimizes excessive partitioning.

An example of how these techniques are leveraged for CPP is provided in [8], where Torres et al. present a method that first computes an optimal line sweep direction to minimize turns and then decomposes concave polygons into convex sub-polygons when a boustrophedon sweep motion is interrupted. Their approach, while effective in reducing the number of turns, follows a more rigid partitioning scheme that over partitions polygons and does not naturally accommodate polygons with holes. In contrast, our method's cost-driven, selective partitioning not only naturally adapts to polygons with holes but also avoids unnecessary subdivisions. Nevertheless, Torres et. al.'s work remains a well established CPP algorithm and thus serves as one of the benchmarks in our evaluation reported in Section V-C.

III. AUTONOMOUS TERRAIN-AWARE MISSION PLANNER

In this work, we develop a two-stage algorithm for terrain-based coverage path planning in SAR scenarios. The first stage is the global planning phase, where CV is used to segment a high-resolution satellite image into terrain-labeled, disjoint rectilinear polygons (see Section IV). The resulting labels and polygons, in conjunction with UAV capabilities and instantaneous positions, are reformulated as a task allocation problem and addressed through a dynamic match-making algorithm (Section IV-B). The second stage consists of a local planning phase, wherein a boustrophedon-based search pattern is used to generate efficient coverage paths within each polygon (see Section IV-A). A key innovation of our approach is the use of a cumulative gap severity metric to guide the partitioning process; intuitively, this metric quantifies the additional distance a standard boustrophedon path would incur due to gaps, holes or concavities of a polygon. Unlike some traditional methods that force cuts at concave (reflex) vertices to enforce monotonicity along a preselected axis, our method relaxes this assumption and only partitions when the polygon is non-monotone in *both* the x - and y -directions.

IV. 2D SCENE RECONSTRUCTION

The mission begins when an operator defines an operational area by creating a bounding box on a map. Let $\Omega \subset \mathbb{R}^2$ denote this search area. We partition Ω into a uniform grid of $N \times M$ cells, where each cell $C_{i,j}$ is defined as

$$C_{i,j} = [x_0 + (j-1)\Delta x, x_0 + j\Delta x) \times [y_0 + (i-1)\Delta y, y_0 + i\Delta y),$$

with (x_0, y_0) representing the lower-left corner of Ω and $\Delta x, \Delta y$ the cell dimensions. A high-resolution satellite image covering Ω is then obtained and processed by a segmentation model $S : \mathbb{R}^3 \rightarrow \{1, 2, 3, \dots\}$ which classifies each pixel into terrain categories (e.g., woodlands, water, buildings, etc.). For each cell $C_{i,j}$, the label is assigned as the terrain category that occupies the largest proportion of pixels in $C_{i,j}$, i.e.,

$$L_{i,j} = \arg \max_{\ell \in \{1, 2, 3, \dots\}} |\{\text{pixels in } C_{i,j} \text{ labeled as } \ell\}|.$$

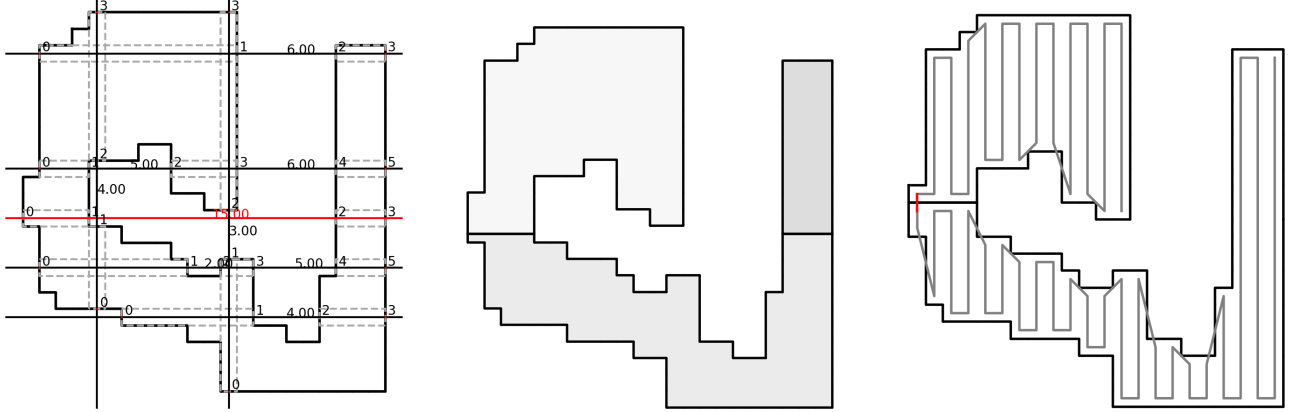


Fig. 2: (left) Polygon overlaid with five horizontal and two vertical sweep lines, with gap evaluations at the intersection points. (middle) Polygon partitions after cut along the sweep line with the highest gap severity. (right) Final boustrophedon coverage path, with red lines indicating the interconnections between individual partition routes.

We then perform a Depth-First Search (DFS) on the labeled cells to identify connected components. Two cells are considered connected if they share a vertical or horizontal boundary and have the same label $L_{i,j}$. This DFS yields a set of connected components $\{\Gamma_1, \Gamma_2, \dots, \Gamma_K\}$. An alternative representation is obtained by converting each Γ_k into a rectilinear polygon by tracing its boundary (possibly with holes). We denote the resulting set of polygons as P_1, P_2, \dots, P_K , where K denotes the number of polygons for the operational scene, Ω . In other words, the Γ and P representations convey the same entity. An example of a reconstructed scene, including the resulting terrain-labeled polygons is shown in Figure 1.

A. Coverage Path Planning on Rectilinear Polygons

Given a rectilinear polygon P obtained from the previous stage, our goal is to compute an efficient coverage path that minimizes the extra distance incurred due to gaps and holes formed due to non-monotonicity. A polygon is said to be *monotone* with respect to a given axis if every line orthogonal to that axis intersects the polygon in a single contiguous segment. Traditional polygon partitioning algorithms often identify concave (reflex) vertices and insert diagonals at these locations to enforce monotonicity in a preselected direction. In contrast, our method permits concavities and triggers partitioning only when P is non-monotone in both the x - and y -directions. We begin by establishing two key criteria. First, we define an *acceptability criterion* for a polygon (or subpolygon): a polygon P is acceptable if it is monotone with respect to at least one coordinate axis, meaning that every candidate sweep line along that axis intersects ∂P in exactly two points. Conversely, if P exhibits concavities in both the x - and y -directions, it fails the acceptability criterion and is deemed *irregular*, indicating that further partitioning is required.

For the sake of completeness, we provide a definition for

monotonicity. To assess monotonicity, let

$$X = \{x_1, x_2, \dots, x_n\} \quad \text{and} \quad Y = \{y_1, y_2, \dots, y_m\}$$

denote the unique x and y coordinates of the vertices of P , respectively. For each candidate sweep line defined at

$$x_c = \frac{x_i + x_{i+1}}{2} \quad \text{or} \quad y_c = \frac{y_j + y_{j+1}}{2},$$

we compute the intersection

$$I(L) = \{p \in \partial P \cap L\}.$$

A monotone polygon yields $|I(L)| = 2$ for every such line; if $|I(L)| > 2$ for a candidate L , this indicates concavity in that direction. If a polygon fails this initial criterion, we then define a *gap severity metric* to determine the optimal partitioning line. For each candidate sweep line exhibiting non-monotonic behavior, we compute a gap severity metric $g(L)$ defined as the cumulative gap between alternating inner intersection points:

$$g(L) = \sum_k \|p_{2k+1} - p_{2k}\|,$$

where $\{p_1, p_2, \dots, p_{|I(L)|}\}$ are the intersection points sorted along the direction of L . This metric serves as a cost function representing the additional traversal penalty that a standard boustrophedon coverage path would incur when traversing through the gaps and/or holes due to non-monotonicity.

Based on this analysis, if P is found to be irregular (i.e., non-monotone in both directions), we select the candidate sweep line L^* with the highest gap severity,

$$L^* = \arg \max_L g(L),$$

and partition P along L^* into sub-polygons $\{P_1, P_2, \dots, P_r\}$. This partitioning process is applied recursively: we first check the polygon (or subpolygon) against the acceptability criterion, and if it fails, we compute the gap severity metric to select a sweep line for partitioning;

the procedure is then repeated on each resulting subpolygon until every subpolygon is acceptable, i.e., monotone with respect to at least one axis. Once the partitioning concludes, the process returns a set of partitioned polygons that satisfy our criterion. However, because the acceptability checks are performed locally on each subpolygon, adjacent sub-polygons may exist whose union would also satisfy the acceptability criterion. To prevent excessive fragmentation, a culling step is performed in which adjacent sub-polygons that share a common boundary segment are merged if their union satisfies the acceptability criterion. We each partition P_i that meets our criteria, we then generate up to eight candidate coverage paths. These candidates arise from different choices of starting corners (four possibilities) and sweep directions (horizontal or vertical); naturally, the criteria may suppress some options, yielding at most eight valid candidates. Note that if a partition is non-monotone in a particular direction, the resulting gaps or holes eliminate some candidate options, so that fewer than eight candidates remain viable. For each partition, we first generate the candidate boustrophedon paths in the allowed directions and then compute their corresponding costs. Each candidate c is represented as a tuple

$$c = (e(c), x(c), c_{\text{int}}(c), \tau(c)),$$

where $e(c)$ and $x(c)$ are the entry and exit points, respectively, expressed as Cartesian coordinates in \mathbb{R}^2 that indicate the start and end positions of the candidate boustrophedon path within P_i . Here, $c_{\text{int}}(c) \in \mathbb{R}$ is the total Euclidean distance traveled along the candidate path within P_i , and $\tau(c) \in \mathbb{N}$ is the number of turns taken along the path.

The cost for each candidate is computed in two parts. First, the internal cost is given by $c_{\text{int}}(c)$. Second, because turns incur additional traversal time (due to deceleration and acceleration), a penalty α is added for each extra turn beyond the minimum turn count among candidates with nearly identical Euclidean costs (within a tolerance ϵ). As stated in [8], [12], for two trajectories of equal length the optimal path in terms of UAV traversal time is the one with the fewest turns (due to deceleration and acceleration costs). We define the adjusted internal cost mathematically as

$$\tilde{c}_{\text{int}}(c) = c_{\text{int}}(c) + \alpha \max \left\{ 0, \tau(c) - \min \left\{ \tau(c') : c' \in \mathcal{C}_i, |c_{\text{int}}(c') - c_{\text{int}}(c)| < \epsilon \right\} \right\}.$$

Let

$$\mathcal{C}_i = \{c_{i,1}, c_{i,2}, \dots, c_{i,k_i}\}$$

denote the set of candidate paths for partition P_i . The next step is global connector optimization, where one candidate is selected from each partition and an ordering of the partitions is determined to minimize the overall traversal cost. The total cost is given by

$$\text{Total Cost} = \sum_{i=1}^N \tilde{c}_{\text{int}}(c_i) + \sum_{i=1}^{N-1} \|x(c_i) - e(c_{i+1})\|,$$

where the second term accounts for the Euclidean distance between the exit point of partition P_i and the entry point of partition P_{i+1} . This global optimization is solved via dynamic programming with bitmasking or [13], for large K number of partitions we implement a greedy heuristic [14].

Finally, once the optimal candidate is selected for each partition and the ordering is determined, the selected candidate paths are concatenated to form a single, continuous global coverage path. Our approach is motivated by the observation that by allowing concavities to remain and partitioning only when a polygon is non-monotone in both directions, we avoid cuts that might otherwise be induced by methods that rigidly enforce monotonicity by cutting at concave vertices. Instead, the chosen partition cut directly corresponds to the region where a conventional boustrophedon path would be most inefficient.

B. Matchmaking Algorithm

As described in Section IV, our algorithm outputs a set of rectilinear terrain polygons $\mathcal{P} = \{P_1, P_2, \dots, P_K\}$, each associated with a terrain type $\tau(P_j) \in \{1, 2, 3, \dots\}$. Let $\mathcal{U} = \{U_1, U_2, \dots, U_{N_u}\}$ denote the set of available UAVs, where each UAV U_i is characterized by a binary capability vector $\mathbf{c}(U_i) \in \{0, 1\}^d$, with d representing the total number of heterogeneous capabilities (payloads, sensors, battery levels, etc.). A terrain prioritization function $\pi : \{1, 2, 3, \dots\} \rightarrow \mathbb{R}^+$ assigns a ranking to the terrain types, with lower values indicating higher priority; since prioritization varies by emergency type, this ranking is provided as an input by the incident operator. Additionally, for each terrain type τ , there is a recommended capability vector $\mathbf{r}(\tau) \in \{0, 1\}^d$ that specifies the ideal capabilities for UAVs to cover that terrain. For example, dense forests or areas with obstacles may require UAVs equipped with lidar or obstacle avoidance systems, whereas water bodies may require thermal sensors or flotation devices. This vector serves as a lookup table that provides recommendations for UAV capabilities based on terrain classification. The assignment problem is to match each UAV to a terrain polygon by considering factors such as capability compatibility, spatial proximity, and terrain priority. This task allocation problem can be addressed

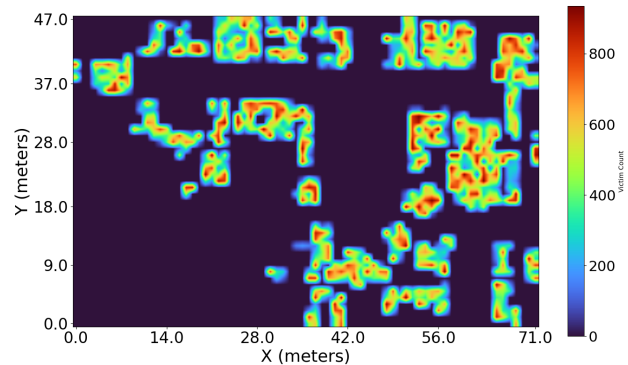


Fig. 3: heat map showing the hot-spots of estimated victim distribution in operational area

through various established approaches [15], such as scoring mechanisms, auction-based algorithms, or linear assignment techniques (e.g., the Hungarian algorithm). This approach handles heterogeneous UAVs, enables flexible terrain-based prioritization, and is inherently robust against uncertain dynamic failures. For example, in the event of a UAV failure, the task can be requeued for another UAV to assume, which contrasts with metaheuristic-based path planners that are designed for offline, static environment, and often require replanning of the entire mission when failures occur.

V. EVALUATION

A. Prototype Implementation

We evaluated our approach in simulation. Hexacopter drones were simulated in Gazebo [16], a high-fidelity physics engine known for its realistic environmental modeling. The drones were controlled using PX4 [17] – a leading open-source Flight Control Unit (FCU), and MAVROS [18] to send commands to UAVs. A 2D user interface built with Angular and Node.js, was used to display real-time operational data, while high-resolution satellite imagery was acquired via the Mapbox API [19]. We analyzed this imagery, using a pretrained DeepLabv3 [20] segmentation model, denoted as $S : \mathbb{R}^3 \rightarrow \{1, 2, 3, \dots\}$ and fine-tuned on the LandCover AI dataset [21], which reconstructs the scene as described in Section IV. This model segments the environment into distinct landcover types such as water bodies, woodlands, roads, and buildings.

B. Case Study: Earthquake Disaster Response

UAV-based SAR are increasingly used for both large-scale disaster relief and missing-person operations, yet they often rely on time-consuming manual terrain analysis to prioritize high-risk areas (e.g., urban collapse zones in earthquakes or linear manmade roads in remote wilderness). In this section, we aim to answer *whether* and *to what extent* incorporating terrain-based landcover information improves the overall victim rescue rate. To this end, we present a case study rooted in state-of-the-art earthquake research. Specifically, we model a magnitude 7 strike-slip earthquake with a vertical fault plane, originating from a hypocenter 15 km underground. The rupture extends across a surface area defined by four corners at depths ranging from 8.26 km to 21.74 km, while the hypocenter is located approximately 32 km from our operational study region. We use the OpenQuake module [23] to compute ground motion fields, asset damage distributions, and building vulnerability curves. Given damage probabilities p_i for each building i from the OpenQuake module, and under the assumption that victims are most likely to be found in the immediate vicinity of compromised structures, we estimate a static victim map via:

$$v_i = o_i \times p_i, \quad (1)$$

where o_i is the an estimated population for building i . Image 3 displays the resulting heat map quantifying victim location in the operational area.

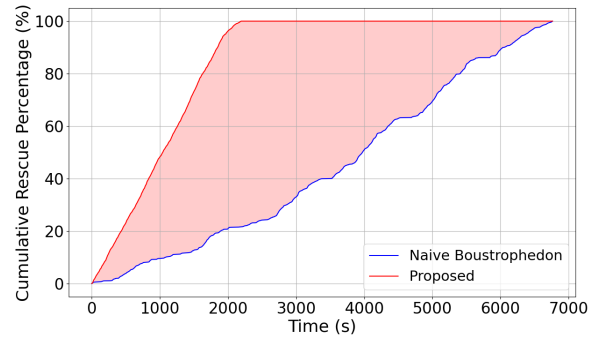


Fig. 4: Cumulative Rescue Curve for Proposed (red) and Naive Boustrophedon (blue) paths

In our experiments, we use the operational area depicted in Image 3, where the only required inputs to our method are (1) a bounding box specifying the latitude–longitude coordinates of the region and (2) a search priority list indicating which landcover types should be prioritized for search (e.g. Buildings). All subsequent terrain segmentation and coverage path generation steps are fully automated by the proposed system. As a baseline, we compare against a *conventional*, non-terrain-aware boustrophedon path that uniformly scans the entire region. This benchmark is well-suited for earthquake scenarios because it is the most efficient path in terms of travel distance and minimal turns.

We configured four drones for both our proposed and baseline system in the Gazebo environment. For each UAV, we recorded the timestamps at which each UAV arrived in a specific grid cell. If a victim was estimated to be in that region (based on the static victim map), we considered the victim to be rescued. From these timestamps, we produced the cumulative rescue curve shown in Figure 4, which denotes the percentage of victims rescued over time.

As depicted, our proposed terrain-aware approach (red curve) achieves a significantly faster rate of victim rescue compared to the conventional, non-terrain-aware boustrophedon method (blue curve). Early in the mission, the red curve rises more steeply which indicates that a larger proportion of victims is located and rescued sooner. By approximately 2,000–3,000 seconds, the proposed method has already rescued the majority of victims, whereas the baseline method requires closer to 4,000–5,000 seconds to reach similar rescue levels. Ultimately, both methods approach complete coverage, but our approach consistently maintains an advantage in rescue percentage at each intermediate time. As a result, our approach not only accelerates victim detection and rescue but also obviates the need for time-consuming manual planning.

C. Comparative Analyzes of Polygon Coverage Path Planning Against Advanced Benchmarks

In the context of UAV-assisted SAR, marginal inefficiencies in local path planning can compound, leading to increased energy consumption and delays in victim rescue. This section evaluates the performance of our proposed *local*

TABLE I: Benchmark Results: Metrics for Each Algorithm on Eight Polygons.

Polygon		Proposed			Torres [8]			NN[14]			GA[22]			DSSA			ACO		
#	S	T	P	R	T	P	R	T	P	R	T	P	R	T	P	R	T	P	R
P_1	277	2408	4.37	66	2538	4.58	68	2780	4.64	127	4730	8.77	169	2967	5.13	107	3147	5.18	169
P_2	158	1433	2.50	51	1486	2.68	40	1501	2.62	48	1977	3.47	78	1577	2.72	45	1662	2.77	80
P_3^*	302	2690	4.75	90	2746 [‡]	5.23 [‡]	36[‡]	2809	5.00	86	4962	8.95	180	3027	5.16	113	3378	5.44	194
P_4^*	684	5726	10.73	104	6728 [‡]	13.07 [‡]	54[‡]	5946	10.88	141	†	40.09	104	9395	16.49	398	8146	13.35	447
P_5	540	4623	8.69	88	4666	8.68	84	4633	8.46	113	13862	26.58	442	6818	11.68	282	6326	10.26	354
P_6	403	3523	6.49	78	3583	6.63	76	3823	6.54	156	8632	16.30	285	4772	8.13	188	4673	7.70	253
P_7	419	3586	6.66	75	3652	6.81	70	3771	6.73	110	8512	15.68	303	4649	7.82	201	4735	7.78	265
P_8^*	403	3469	6.25	96	4395 [‡]	8.46 [‡]	48[‡]	3707	6.50	125	8592	16.09	288	4602	8.01	178	4582	7.52	247

notes: Best value for each performance metric are **bolded**. ^{*}: Indicates polygon contains holes. [‡]: Indicates that the algorithm is unable to process polygons with holes; the reported value corresponds to the polygon after holes have been filled. [†]: Simulation omitted as the algorithm produced an excessively long path, rendering it impractical. S =number of constituent cells in P . T = Time (s), P = Path Length (m), R = Turns; Algorithm acronyms: NN = Nearest Neighbor, GA = Genetic Algorithm, DSSA = Direct Search Simulated Annealing, ACO = Ant Colony Optimization.

TABLE II: Parameter Settings

		Parameter	Value
Algorithm Related	DSSA	N	100
		T_{\max}	30000
		p_D	0.2
		p_δ	0.1
	ACO	m	40
		T_{\max}	600
		α	1.0
		β	2.5
		ρ	0.15
	GA	Q	100.0
		τ_0	1.0
Scene Related		N	300
		G	2000
		p_c	0.9
		p_m	0.3
	(Δ x , Δ y)		(15,15)
	v	2	

Notation: **DSSA**: N = Population size, T_{\max} = Max. iterations, p_D = Discoverers probability, p_δ = Danger probability; **ACO**: m = No. of ants, T = Max. iterations, α = Pheromone influence, β = Heuristic influence, ρ = Evaporation rate, Q = Deposit factor, τ_0 = Initial pheromone; **GA**: N = Population size, G = No. of generations, p_c = Crossover rate, p_m = Mutation rate. $(\Delta x, \Delta y)$ = cell size, v = Drone velocity (m/s)

coverage path planning algorithm described in Section IV-A. Given a set of rectilinear polygons P composed of equi-sized constituent cells, the objective is to compute a path that visits each cell at least once while minimizing total travel time—in other words, a Hamiltonian path. For benchmarking, we compare our method against five well-established baseline algorithms: three metaheuristic approaches—Ant Colony Optimization (ACO), Dynamic Self-Organizing Swarm Algorithm (DSSA), and Genetic Algorithm (GA)—along with a nearest neighbor heuristic (NN) and the Torres et al. [8] algorithm implemented using MATLAB’s UAV module [24].

Evaluation is conducted on a suite of challenging non-monotonic and irregular rectilinear polygons, some of which contain holes and exhibit multiple concavity points. Each cell C in P has a fixed size of 15×15 . Simulations are performed in Gazebo with hexacopter UAVs operating at

a fixed velocity. In UAV operations, completion time is influenced not only by the overall path length but also by the number of turns, as each turn necessitates deceleration and subsequent re-acceleration [8] [12], which ultimately incurs additional temporal and energy costs. Consequently, our evaluation measures the total path length, the number of turns, and the overall completion time for each polygon. For the meta-heuristic benchmarks, we minimize the following objective function:

$$J(r) = \sum_{i=1}^{n-1} \|r_{i+1} - r_i\| + \lambda T(r),$$

where $\|r_{i+1} - r_i\|$ represents the Euclidean distance between two cells in the ordered path $r = \{r_1, r_2, \dots, r_n\}$, $T(r)$ is the number of turns in the path, and λ is a tunable parameter that penalizes turning. we set $\lambda = 1$ so that the Euclidean distance is the dominant contributing factor in the objective function. For the metaheuristic algorithms (GA, DSSA, and ACO), we set T_{\max} to a generous 15-minute limit per polygon. This allows sufficient iterations to generate quality coverage paths while adhering to the real-time constraints of SAR operations. Table II provides relevant parameter settings.

Table I illustrates the raw performance metrics, namely: completion time T , path length P and number of turns R . Our method consistently yields the lowest completion times across all polygons. Ranking the algorithms by performance, our proposed method is best, followed by the Torres et al. approach, with the Nearest Neighbor (NN) heuristic ranking third. Notably, the metaheuristic models (GA, DSSA, ACO) incur significantly longer completion times. While the Torres method often achieves paths with fewer turns, our algorithm’s focus on generating a minimal candidate subset leads to shorter overall path lengths. This reduction in path length directly translates to optimal time completions while keeping the number of turns at a level comparable to that of Torres. In contrast, the NN heuristic, despite achieving similar path lengths to our approach, exhibits nearly double the number of turns per polygon.

Table III demonstrates the relative time completion speed

up our proposed algorithm would yield compared to the established benchmarks, defined as Speedup = $\frac{T_{\text{benchmark}}}{T_{\text{proposed}}}$. Our method demonstrates improvements of up to 26% and 15% relative to the second and third best benchmark models, respectively. These gains are particularly significant when extrapolated to a scenario where say 1kmx1km scene potentially compromises of hundreds of polygons. The compounded effect of these improvements could lead to more efficient global searches in large-scale missions.

TABLE III: Relative Speedup of Our Algorithm Compared to Benchmarks on Eight Polygons

Polygon	Torres [8]	NN [14]	GA[22]	DSSA	ACO
P_1	1.0541	1.1545	1.9645	1.2323	1.3072
P_2	1.0371	1.0475	1.3797	1.1004	1.1601
P_3^*	1.0208	1.0444	1.8448	1.1254	1.2558
P_4^*	1.1749	1.0384	†	1.6406	1.4225
P_5	1.0093	1.0023	2.9987	1.4749	1.3684
P_6	1.0172	1.0854	2.4506	1.3547	1.3266
P_7	1.0185	1.0517	2.3738	1.2964	1.3205
P_8^*	1.2669	1.0686	2.4772	1.3268	1.3210

Footnotes: *: Indicates polygon contains holes. †: Simulation omitted as the algorithm produced an excessively long path, rendering it impractical

VI. CONCLUSION

In this paper, we presented a novel terrain-aware mission planning framework designed to enhance UAV-assisted search and rescue operations. By leveraging deep segmentation techniques on high-resolution satellite imagery, our method automatically extracts and analyzes landcover features to partition the operational area into terrain-specific regions. These regions are subsequently allocated among heterogeneous UAVs via a task matchmaking algorithm which alleviates the need for manual pre-flight planning that is traditionally human-driven.

We have also introduced a novel coverage path planner for rectilinear polygons. A key contribution of our approach is a recursive polygon decomposition strategy that selectively partitions regions based on a gap severity metric, followed by a merging procedure to consolidate adjacent sub-polygons whose union satisfies the acceptability criterion and a dynamic programming approach to optimize the overall candidate paths and minimize turns in a boustrophedon path. This approach improves mission completion times by considerable margins (up to 26% with respect to the second best baseline) and outperforms all other presented heuristics and meta-heuristic baselines.

REFERENCES

- [1] B. Li, S. Patankar, B. Mordian, and N. Mahmoudian, “Planning large-scale search and rescue using team of uavs and charging stations,” in *2018 IEEE International Symposium on Safety, Security, and Rescue Robotics (SSRR)*, 2018, pp. 1–8.
- [2] S. Hayat, E. Yannaz, C. Bettstetter *et al.*, “Multi-objective drone path planning for search and rescue with quality-of-service requirements,” *Autonomous Robots*, vol. 44, pp. 1183–1198, 2020. [Online]. Available: <https://doi.org/10.1007/s10514-020-09926-9>
- [3] M. Morin, I. Abi-Zeid, and C.-G. Quimper, “Ant colony optimization for path planning in search and rescue operations,” *European Journal of Operational Research*, vol. 305, no. 1, pp. 53–63, 2023. [Online]. Available: <https://www.sciencedirect.com/science/article/pii/S0377221722004945>
- [4] Q. Meng, K. Chen, and Q. Qu, “Ppswarm: Multi-uav path planning based on hybrid pso in complex scenarios,” *Drones*, vol. 8, no. 5, 2024. [Online]. Available: <https://www.mdpi.com/2504-446X/8/5/192>
- [5] D. Li, W. Yin, W. Wong, M. Jian, and M. Chau, “Quality-oriented hybrid path planning based on a* and q-learning for unmanned aerial vehicle,” *IEEE Access*, vol. PP, pp. 1–1, 12 2021.
- [6] M. Jacobs, “Terrain based probability models for sar,” *San Diego: Mountain Rescue*, 2015.
- [7] H. Choset and P. Nignon, “Coverage path planning: The boustrophedon cellular decomposition,” in *Field and service robotics*. Springer, 1998, pp. 203–209.
- [8] M. Torres, D. A. Pelta, J. L. Verdegay, and J. C. Torres, “Coverage path planning with unmanned aerial vehicles for 3d terrain reconstruction,” *Expert Systems with Applications*, vol. 55, pp. 441–451, 2016. [Online]. Available: <https://www.sciencedirect.com/science/article/pii/S0957417416300306>
- [9] Ghambari, Soheila, Golabi, Mahmoud, Jourdan, Laetitia, Lepagnot, Julien, and Idoumghar, Lhassane, “Uav path planning techniques: a survey,” *RAIRO-Oper. Res.*, vol. 58, no. 4, pp. 2951–2989, 2024. [Online]. Available: <https://doi.org/10.1051/ro/2024073>
- [10] I. Chaari, A. Koubaa, H. Bennaceur, A. Ammar, M. Alajlan, and H. Youssef, “Design and performance analysis of global path planning techniques for autonomous mobile robots in grid environments,” *International Journal of Advanced Robotic Systems*, vol. 14, 04 2017.
- [11] E. Galceran and M. Carreras, “A survey on coverage path planning for robotics,” *Robotics and Autonomous Systems*, vol. 61, no. 12, pp. 1258–1276, 2013. [Online]. Available: <https://www.sciencedirect.com/science/article/pii/S092188901300167X>
- [12] Y. Li, H. Chen, M. Joo Er, and X. Wang, “Coverage path planning for uavs based on enhanced exact cellular decomposition method,” *Mechatronics*, vol. 21, no. 5, pp. 876–885, 2011, special Issue on Development of Autonomous Unmanned Aerial Vehicles. [Online]. Available: <https://www.sciencedirect.com/science/article/pii/S0957415810001893>
- [13] M. Held and R. M. Karp, “A dynamic programming approach to sequencing problems,” *Journal of the Society for Industrial and Applied mathematics*, vol. 10, no. 1, pp. 196–210, 1962.
- [14] E. L. Lawler, “The traveling salesman problem: a guided tour of combinatorial optimization,” *Wiley-Interscience Series in Discrete Mathematics*, 1985.
- [15] S. Alqefari and M. Menai, “Multi-uav task assignment in dynamic environments: Current trends and future directions,” *Drones*, vol. 9, no. 1, p. 75, 2025.
- [16] N. Koenig and A. Howard, “Design and use paradigms for gazebo, an open-source multi-robot simulator,” in *2004 IEEE/RSJ International Conference on Intelligent Robots and Systems (IROS) (IEEE Cat. No.04CH37566)*, vol. 3, 2004, pp. 2149–2154 vol.3.
- [17] PX4, “Px4 autopilot,” <https://github.com/PX4/PX4-Autopilot>, accessed: 2025-04-15.
- [18] V. Ermakov, “MAVROS.” [Online]. Available: <https://github.com/mavlink/mavros>
- [19] Mapbox, “Mapbox api documentation,” <https://docs.mapbox.com/api/overview/>, 2025, accessed: 2025-02-15.
- [20] L.-C. Chen, G. Papandreou, F. Schroff, and H. Adam, “Rethinking atrous convolution for semantic image segmentation,” 2017.
- [21] A. Boguszewski, D. Batorski, N. Ziembka-Jankowska, T. Dziedzic, and A. Zambrzycka, “Landeover.ai: Dataset for automatic mapping of buildings, woodlands, water and roads from aerial imagery,” in *Proceedings of the IEEE/CVF Conference on Computer Vision and Pattern Recognition (CVPR) Workshops*, June 2021, pp. 1102–1110.
- [22] J. Tu and S. Yang, “Genetic algorithm based path planning for a mobile robot,” in *2003 IEEE International Conference on Robotics and Automation (Cat. No.03CH37422)*, vol. 1, 2003, pp. 1221–1226 vol.1.
- [23] Global Earthquake Model (GEM), “Openquake engine,” <https://github.com/gem/oq-engine>, 2013, accessed: 5 February 2025.
- [24] MathWorks, “uavCoveragePlanner,” 2023, computer software. [Online]. Available: <https://www.mathworks.com/help/uav/ref/uavcoverageplanner.html>